Inorg. Chem. **2006**, *45*, 5172–5178

$Ce_{53}Fe_{12}S_{90}X_3$ (X = Cl, Br, I): The First Rare-Earth Transition-Metal Sulfide Halides

Allison M. Mills and Michael Ruck*

Institut für Anorganische Chemie, Technische Universität Dresden, D-01062 Dresden, Germany

Received December 14, 2005

The compounds $Ce_{53}Fe_{12}S_{90}X_3$ (X = Cl, Br, I), which represent the first examples of rare-earth transition-metal sulfide halides, were prepared using the reactive-flux method, through reaction of Ce_2S_3, FeS, or Fe and S in a CeX_3 flux at 1320 K. Their structures were determined by single-crystal X-ray diffraction. The compounds are isostructural, crystallizing in the trigonal space group $R\bar{3}m$ with $Z = 1$ [$Ce_{53}Fe_{12}S_{90}Cl_3$, $a = 13.9094(9)$ Å, $c = 21.604(2)$ Å, $V = 3619.7(4)$ Å^3; $Ce_{53}Fe_{12}S_{90}Br_3$, $a = 13.916(1)$ Å, $c = 21.824(2)$ Å, $V = 3660.0(5)$ Å^3; $Ce_{53}Fe_{12}S_{90}I_3$, $a = 13.863(3)$ Å, $c = 21.944(6)$ Å, $V = 3652(2)$ Å^3]. The structure adopted is a stuffed variant of the $La_{52}Fe_{12}S_{90}$ structure type. Fe_2S_9 dimers of face-sharing octahedra are linked by face- and vertex-sharing capped CeS_6 trigonal prisms, forming a three-dimensional framework containing cuboctahedral cavities of two sizes. The smaller cavities accommodate alternative sites for disordered cerium atoms. The larger cavities, which remain empty in the parent structure, are filled by halogen atoms in $Ce_{53}Fe_{12}S_{90}X_3$. Alternatively, the structure can be described as a 9-fold superstructure of the Mn_5Si_3 structure type ($P6_3/mcm$), with $a = \sqrt{3}a'$ and $c = 3c'$. Temperature-dependent magnetic susceptibility measurements suggest that $Ce_{53}Fe_{12}S_{90}I_3$ may order antiferromagnetically at low temperatures.

Introduction

We have recently undertaken a reinvestigation of the ternary R−Fe−S system (R = rare-earth metal), with the goal of developing structure−property relationships for these mixed-metal compounds. Within this system, phases with compositions $R_2Fe_{2-\delta}S_5$ (R = La, Ce, Pr), $R_3Fe_{2-\delta}S_7$ (R = La, Ce, Pr, Nd; also formerly referred to as R_4FeS_7), and $R_{52}Fe_{12}S_{90}$ (R = La, Ce, Pr, Nd; also formerly referred to as R_2FeS_4 or $R_{32.66}Fe_{11}S_{60}$) have been reported for the larger rare-earth metals.[1−3] All possess crystal structures featuring FeS_n polyhedra that are either isolated or condensed into dimers or chains.[4−9] These low-dimensional units are interconnected by trivalent rare-earth cations, allowing for complex magnetic coupling interactions involving the iron $3d^n$ and rare-earth $4f^n$ moments. However, the magnetic properties of the compounds containing nonmagnetic La^{III} ions have been the most thoroughly studied to date.[10−14] Our main interest lies in the phase-pure preparation and structural and magnetic characterization of the latter (magnetic-moment-bearing) rare-earth analogues.

The $R_{52}Fe_{12}S_{90}$ compounds adopt what was originally known as the $La_{32.66}Mn_{11}S_{60}$ structure type;[8] however, the formula and structure have undergone several revisions. The compounds "R_2FeS_4" (R = La, Ce) were discovered in 1968, and their monoclinic cell parameters were reported at that time.[2] The crystal structure of "$La_{32.66}Fe_{11}S_{60}$" was then

* To whom correspondence should be addressed. E-mail: michael.ruck@chemie.tu-dresden.

(1) Collin, G.; Rouyer, F.; Loriers, J. *C. R. Acad. Sci., Ser. C* **1968**, *266*, 689−691.
(2) Patrie, M.; Nguyen, H.-D.; Flahaut, J. *C. R. Acad. Sci., Ser. C* **1968**, *266*, 1575−1578.
(3) Du, Y.; Tang, G. *Huaxue Tongbao* **1984**, *2*, 18−19.
(4) Besrest, F.; Collin, G. *J. Solid State Chem.* **1977**, *21*, 161−170.
(5) Besrest, F.; Collin, G. *J. Solid State Chem.* **1978**, *24*, 301−309.
(6) Harms, W.; Mills, A. M.; Söhnel, T.; Laubschat, C.; Wagner, F. E.; Geibel, C.; Hossain, Z.; Ruck, M. *Solid State Sci.* **2005**, *7*, 59−66.
(7) Mills, A. M.; Ruck, M. *Acta Crystallogr., Sect. C* **2004**, *60*, i71−i72.
(8) Collin, G.; Laruelle, P. *Acta Crystallogr., Sect. B* **1974**, *30*, 1134−1139.
(9) Mills, A. M.; Bräunling, D.; Ruck, M. *Acta Crystallogr., Sect. C*, in press.
(10) Collin, G.; Barthélémy, É.; Gorochov, O. *C. R. Acad. Sci., Ser. C* **1973**, *277*, 775−778.
(11) Plumier, R.; Sougi, M.; Collin, G. *Solid State Commun.* **1974**, *14*, 971−973.
(12) Plumier, R.; Sougi, M.; Lecomte, M. *J. Appl. Phys.* **1981**, *52*, 2320−2322.
(13) Plumier, R.; Lecomte, M.; Collin, G.; Keller-Besrest, F. *Phys. Lett., Sect. A* **1980**, *76*, 419−420.
(14) Nanjundaswamy, K. S.; Gopalakrishnan, J. *J. Solid State Chem.* **1983**, *49*, 51−58.

10.1021/ic0521372 CCC: $33.50
Published on Web 05/24/2006

determined in the nonstandard monoclinic space group *Bm*,[8] but it was later noted that trigonal symmetry had been overlooked.[15] We recently redetermined the structure in $R\bar{3}m$ and suggested the new formula $La_{52}Fe_{12}S_{90}$.[9] In the structure, which is related to the prevalent Mn_5Si_3 structure type,[16] Fe_2S_9 dimers and large cuboctahedral cavities alternate along the $\bar{3}$ axes. Given the extensive interstitial chemistry of the Mn_5Si_3-type phases, which has been studied in detail by Corbett and co-workers,[17] we anticipated that it would be possible to form a stuffed version of the $La_{52}Fe_{12}S_{90}$ structure by filling the cavities. In $Ce_{53}Fe_{12}S_{90}X_3$ (X = Cl, Br, I), halide anions have been incorporated into a $La_{52}Fe_{12}S_{90}$-type host to give the first examples of rare-earth transition-metal sulfide halides.

Experimental Section

Synthesis. Ce_2S_3, CeX_3 (X = Cl, Br, I; anhydrous beads, 99.9%, Aldrich), Fe (powder, 99.9%, ABCR; reduced with H_2 at 770 K), FeS, and S (powder, >99%, VEB Laborchemie; recrystallized from CS_2 and then purified of carbon according to the method of von Wartenberg[18]) were used as starting materials. Ce_2S_3 was synthesized by reacting stoichiometric amounts of Ce (rod, >99.5%, Treibacher; freshly filed under argon prior to use) and S at 1370 K. FeS was prepared by reacting stoichiometric amounts of Fe and S at 1170 K.

Crystals of the sulfide chloride $Ce_{53}Fe_{12}S_{90}Cl_3$ were first isolated from a reaction in a $CeCl_3$ flux, according to the method reported for the preparation of the structurally related compound $La_{15.9}Cr_{5.4}S_{32}$.[19] The starting reactants Ce_2S_3, Fe, and S, in a ratio of 3:2.5:2.7 (0.25 g in total), were combined with the $CeCl_3$ flux (20 wt %) in a glassy-carbon crucible contained within a fused-silica ampule (12-cm length and 1.5-cm diameter). The ampule was sealed under vacuum (10^{-3} Torr), then heated at 1320 K for 2 days, and subsequently quenched in air. The excess flux was removed by washing the sample several times with ethanol. Similar reactions of Ce_2S_3, FeS, and S, in a ratio of 3:2:1, in a $CeBr_3$ or CeI_3 flux produced crystals of the bromide and iodide analogues. The resulting products contained black multifaceted crystals of the sulfide halides. Energy-dispersive X-ray spectroscopic analyses of the crystals on a Zeiss DSM 982 Gemini scanning electron microscope confirmed the presence of the four component elements in the appropriate ratios, within experimental error.

Structure Determination. Analysis of the products by powder X-ray diffraction on a Siemens D5000 diffractometer revealed that the major phases, $Ce_{53}Fe_{12}S_{90}Cl_3$, $Ce_{53}Fe_{12}S_{90}Br_3$, and $Ce_{53}Fe_{12}S_{90}I_3$, adopt a structure related to the $La_{52}Fe_{12}S_{90}$ type.[8,9] While the $Ce_{53}Fe_{12}S_{90}I_3$ sample was essentially phase pure (to the detection limits), the other samples contained varying amounts of $Ce_{10}S_{14}O$[20] and FeS.[21] The cell parameters of the three $Ce_{53}Fe_{12}S_{90}X_3$ phases, refined by least-squares methods from their powder patterns indexed in $R\bar{3}m$, using the program *UNITCELL*,[22] are plotted in Figure 1.

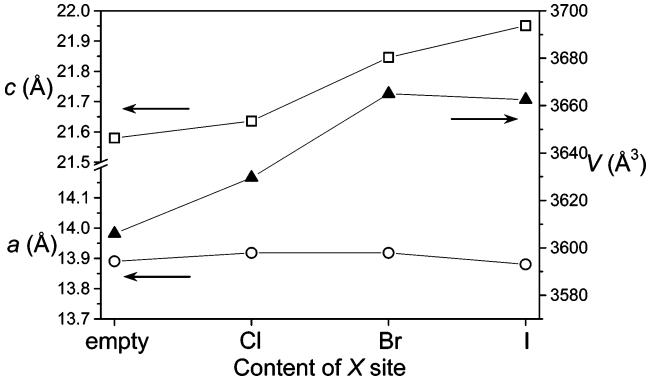

Figure 1. Variation of the cell parameters of $Ce_{53}Fe_{12}S_{90}X_3$ (X = Cl, Br, I) with the size of X. The cell parameters of $Ce_{52}Fe_{12}S_{90}$, in which the X site is empty, are also plotted for comparison.

Table 1. Crystallographic Data for $Ce_{53}Fe_{12}S_{90}X_3$ (X = Cl, Br, I)

formula	$Ce_{53}Fe_{12}S_{90}Cl_3$	$Ce_{53}Fe_{12}S_{90}Br_3$	$Ce_{53}Fe_{12}S_{90}I_3$
fw	11 088.31	11 221.69	11 362.66
space group	$R\bar{3}m$ (No. 166)	$R\bar{3}m$ (No. 166)	$R\bar{3}m$ (No. 166)
a (Å)	13.9094(9)	13.916(1)	13.863(3)
c (Å)	21.604(2)	21.824(2)	21.944(6)
V (Å^3)	3619.7(4)	3660.0(5)	3652(2)
Z	1	1	1
T (K)	293	293	293
λ (Å)	0.71073	0.71073	0.71073
D_{calcd} (g cm^{-3})	5.09	5.09	5.17
μ(Mo Kα) (cm^{-1})	188	193	192
R1 [$F_o > 4\sigma(F_o)$]^a	0.045	0.032	0.033
wR2 (all F_o^2)^b	0.120	0.078	0.078

^{a} $R1 = \sum||F_o| - |F_c||/\sum|F_o|$. ^{b} $wR2 = [\sum w(F_o^2 - F_c^2)^2/\sum wF_o^4]^{1/2}$.

The cell parameters of the parent compound $Ce_{52}Fe_{12}S_{90}$, calculated from the monoclinic cell parameters reported for "Ce_2FeS_4", are also plotted for comparison.[2,15]

Single-crystal X-ray diffraction experiments confirmed that the sulfide halides are filled derivatives of $Ce_{52}Fe_{12}S_{90}$. Intensity data for crystals of $Ce_{53}Fe_{12}S_{90}Cl_3$, $Ce_{53}Fe_{12}S_{90}Br_3$, and $Ce_{53}Fe_{12}S_{90}I_3$ were collected at 293 K using graphite-monochromated Mo Kα radiation, on a Stoe IPDS-II diffractometer. Numerical absorption corrections were applied with the program *X-RED*,[23] based on crystal descriptions optimized using equivalent reflections with the program *X-SHAPE*.[24] Crystal data and further details of the data collections are given in Table 1. In all three cases, a trigonal cell was found, and intensity statistics were consistent with Laue symmetry $\bar{3}m$. For the $Ce_{53}Fe_{12}S_{90}I_3$ crystal, the systematic reflection condition for R-centering (*hkl*: $-h + k + l = 3n$, obverse setting) was clearly obeyed; however, for the $Ce_{53}Fe_{12}S_{90}Cl_3$ and $Ce_{53}Fe_{12}S_{90}Br_3$ crystals, some reflections (with $l \neq 3n$) violated this condition, indicating obverse/reverse twinning. No additional reflection conditions were observed. The centrosymmetric space group $R\bar{3}m$ was therefore chosen on the basis of the close relationship between the structures of $Ce_{53}Fe_{12}S_{90}X_3$ and $La_{52}Fe_{12}S_{90}$.[9]

For simplicity, the structure of the untwinned $Ce_{53}Fe_{12}S_{90}I_3$ crystal was examined first. The structure was solved by direct methods using *SHELXS97* and refined on F^2 using *SHELXL97*.[25] After three cerium, two iron, and five sulfur sites were located, additional electron density remained within two types of large

(15) Cenzual, K.; Gelato, L. M.; Penzo, M.; Parthé, E. *Z. Kristallogr.* **1990**, *193*, 217−242.
(16) Åmark, K.; Boren, B.; Westgren, A. *Sven. Kem. Tidskr.* **1936**, *48*, 273−276.
(17) Corbett, J. D.; Garcia, E.; Guloy, A. M.; Hurng, W.-M.; Kwon, Y.-U.; Leon-Escamilla, E. A. *Chem. Mater.* **1998**, *10*, 2824−2836.
(18) von Wartenberg, H. *Z. Anorg. Allg. Chem.* **1956**, *286*, 243−246.
(19) Litteer, J. B.; Sirchio, S. A.; Fettinger, J. C.; Smolyaninova, V.; Eichhorn, B. W.; Greene, R. L. *Chem. Mater.* **1999**, *11*, 1179−1182.
(20) Schleid, T.; Lissner, F. *J. Less-Common Met.* **1991**, *175*, 309−319.
(21) King, H. E., Jr.; Prewitt, C. T. *Acta Crystallogr., Sect. B* **1982**, *38*, 1877−1887.
(22) Holland, T. J. B.; Redfern, S. A. T. *Mineral. Magn.* **1997**, *61*, 65−77.
(23) *X-RED*, version 1.22; Stoe & Cie: Darmstadt, Germany, 2001.
(24) *X-SHAPE*, version 1.06; Stoe & Cie: Darmstadt, Germany, 1999.
(25) Sheldrick, G. M. *SHELX97*; Universität Göttingen: Göttingen, Germany, 1997.

Table 2. Positional and Displacement Parameters for Prototypical $Ce_{53}Fe_{12}S_{90}I_3$

atom	Wyckoff	occupancy	*x*	*y*	*z*	U_{iso}/U_{eq} [a] (Å^2)
Ce(1a)	18h	0.166(6)	0.1388(2)	0.2776(4)	0.3805(4)	0.0164(3)
Ce(1b)	18h	0.35(3)	0.1283(5)	0.257(1)	0.4030(8)	0.0164(3)
Ce(1c)	18h	0.27(3)	0.1217(4)	0.2433(8)	0.4138(6)	0.0164(3)
Ce(1d)	18h	0.028(7)	0.072(2)	0.144(5)	0.445(2)	0.0164(3)
Ce(1e)	18h	0.036(7)	0.085(2)	0.170(4)	0.455(2)	0.0164(3)
Ce(1f)	18h	0.021(2)	0.075(2)	0.149(3)	0.478(2)	0.0164(3)
Ce(1g)	18h	0.058(2)	0.0460(5)	0.092(1)	0.4950(4)	0.0164(3)
Ce(1h)	3b	0.079(4)	0	0	$^1/_2$	0.0164(3)
Ce(2)	18h	1	0.46973(2)	0.53027(2)	0.41137(2)	0.0146(2)
Ce(3)	18h	1	0.53652(2)	0.46348(2)	0.23889(2)	0.0145(2)
Fe(1)	6c	1	0	0	0.1881(1)	0.0199(5)
Fe(2)	6c	1	0	0	0.3285(1)	0.0229(6)
S(1)	18h	1	0.4195(1)	0.5805(1)	0.2813(2)	0.0397(8)
S(2)	18h	1	0.5792(1)	0.4208(1)	0.0721(1)	0.0255(6)
S(3)	18h	1	0.7561(1)	0.2439(1)	0.2004(1)	0.0160(5)
S(4)	18g	1	0.2925(3)	0	$^1/_2$	0.0378(8)
S(5)	18f	1	0.2955(2)	0	0	0.0184(5)
I	3a	1	0	0	0	0.0382(5)

[a] For Ce(1a−h), the values given are the isotropic displacement parameters (U_{iso}), while for all other atoms, they are the equivalent displacement parameters (U_{eq}), defined as one-third of the trace of the orthogonalized $\mathbf{U}_{ij}$ tensor.

cuboctahedral cavities. A site at (0, 0, 0), at the center of the larger cavity, was assigned to iodine. A series of closely spaced sites extend from the center of the smaller cavity at (0, 0, $^1/_2$) to one cerium atom of the surrounding framework. These were attributed to a positional disorder of the cerium atom. The eight split positions Ce(1a−h) were refined with the same isotropic displacement parameter. All other atoms were refined with anisotropic displacement parameters. Free refinement of the occupancies of sites Ce(1a−h) resulted in a total occupancy of 0.92(5), in agreement with the occupancy of $^{17}/_{18}$ required for charge balance according to the formula $(Ce^{3+})_{53}\square_1(Fe^{2+})_{12}(S^{2-})_{90}(I^-)_3$. In later refinements, the occupancies were constrained to sum to this value. The possibility of reduced occupancy of the iron sites was also explored. Refinement of the occupancies of Fe(1) and Fe(2) resulted in values of 0.95(1) and 1.00(1), respectively. The small departure from full occupancy for Fe(1), which lies at a high symmetry site, is likely a result of systematic errors[26] and related with the disorder in the structure. Therefore, we consider the iron sites to be fully occupied, consistent with the formula $Ce_{53}Fe_{12}S_{90}I_3$.

The two remaining structures were solved and refined in a similar manner. In these cases, the smaller halogen atoms are displaced from the center of the larger cavity to a lower symmetry 18h site, which is $^1/_6$ occupied. Fourier maps of the cavities, generated with the program *WinGX*,[27] showed that the electron density associated with the halogen atoms has distinct lobes in the directions of the six 18h sites and is significantly reduced at the central 3a site. The disordered X sites were refined with isotropic displacement parameters. As mentioned above, the crystals of $Ce_{53}Fe_{12}S_{90}Cl_3$ and $Ce_{53}Fe_{12}S_{90}Br_3$ were obverse/reverse twins, with the refined relative fractional contributions of the twin components being 0.688:0.312(6) and 0.935:0.065(5), respectively. Final values of the positional and displacement parameters for prototypical $Ce_{53}Fe_{12}S_{90}I_3$ are given in Table 2. Selected interatomic distances for all three structures are listed in Table 3. Further data, in the form of CIFs, are available as Supporting Information. Graphics were prepared using the program *DIAMOND*.[28]

Magnetic Measurements. Magnetic susceptibility measurements were made on a powder sample of $Ce_{53}Fe_{12}S_{90}I_3$ (ca. 13 mg), using a Quantum Design MPMS XL-7 SQUID magnetometer. The sample magnetization was measured from 2 to 400 K at fields of 0.01−7 T. The measurements were hampered by the presence of a ferromagnetic impurity with a high Curie temperature (T_C > 400 K) and a magnetization corresponding to approximately 100 ppm (by mass) of iron metal. The high-field measurements minimize the influence of the impurity, and the data from these measurements were used in all calculations.

Table 3. Selected Interatomic Distances (Å) in $Ce_{53}Fe_{12}S_{90}X_3$ (X = Cl, Br, I)

	$Ce_{53}Fe_{12}S_{90}Cl_3$	$Ce_{53}Fe_{12}S_{90}Br_3$	$Ce_{53}Fe_{12}S_{90}I_3$
Ce(1b)[a]−S(1) × 2	2.77(1)	2.787(8)	2.747(6)
Ce(1b)[a]−S(2)	2.78(2)	2.78(1)	2.82(1)
Ce(1b)[a]−S(2)	3.18(3)	3.16(2)	3.26(2)
Ce(1b)[a]−S(4) × 2	3.02(2)	3.04(2)	2.97(1)
Ce(1b)[a]−S(5) × 2	3.31(2)	3.29(2)	3.35(1)
Ce(2)−S(1)	3.098(6)	3.131(4)	3.098(4)
Ce(2)−S(2) × 2	2.869(1)	2.8823(8)	2.8765(9)
Ce(2)−S(3)	2.874(4)	2.853(3)	2.848(2)
Ce(2)−S(3)	2.920(4)	2.914(3)	2.912(2)
Ce(2)−S(4) × 2	3.488(5)	3.492(3)	3.547(3)
Ce(2)−S(5) × 2	2.9241(6)	2.9382(5)	2.9192(7)
Ce(3)−S(1)	2.952(5)	2.981(3)	2.961(3)
Ce(3)−S(2)	3.727(5)	3.830(3)	3.800(3)
Ce(3)−S(3) × 2	2.868(1)	2.877(1)	2.895(1)
Ce(3)−S(4) × 2	2.9096(8)	2.9456(5)	2.9139(7)
Ce(3)−S(5) × 2	2.934(2)	2.933(2)	2.944(1)
Ce(3)−X[b]	3.17(3)/3.48(2)	3.332(9)/3.520(7)	3.7497(9)
Fe(1)−S(2) × 3	2.630(5)	2.667(4)	2.641(3)
Fe(1)−S(3) × 3	2.476(4)	2.468(3)	2.466(3)
Fe(2)−S(1) × 3	2.429(6)	2.421(4)	2.414(4)
Fe(2)−S(2) × 3	2.602(6)	2.567(4)	2.567(3)

[a] The Ce(1b) site is one of eight possible sites for Ce(1) and has an occupancy of 26(3)% in $Ce_{53}Fe_{12}S_{90}Cl_3$, 28(3)% in $Ce_{53}Fe_{12}S_{90}Br_3$, and 35(3)% in $Ce_{53}Fe_{12}S_{90}I_3$. [b] The X atoms in $Ce_{53}Fe_{12}S_{90}Cl_3$ and $Ce_{53}Fe_{12}S_{90}Br_3$ are disordered over six symmetry-related positions that are each $^1/_6$ occupied, resulting in four different Ce(3)−X distances, two of which are reasonable bond lengths.

Results and Discussion

Structure Description. The three sulfide halides $Ce_{53}Fe_{12}S_{90}Cl_3$, $Ce_{53}Fe_{12}S_{90}Br_3$, and $Ce_{53}Fe_{12}S_{90}I_3$ all adopt the same structure, which is a stuffed variant of the $La_{52}Fe_{12}S_{90}$ structure type.[8,9] $Ce_{53}Fe_{12}S_{90}I_3$ is used as an example for its description below. As shown in Figure 2,

(26) Guloy, A. M.; Corbett, J. D. *Inorg. Chem.* **1996**, *35*, 4669−4675.
(27) Farrugia, L. J. *J. Appl. Crystallogr.* **1999**, *32*, 837−838.
(28) Brandenburg, K. *DIAMOND*, version 2.1c; Crystal Impact: Bonn, Germany, 1999.

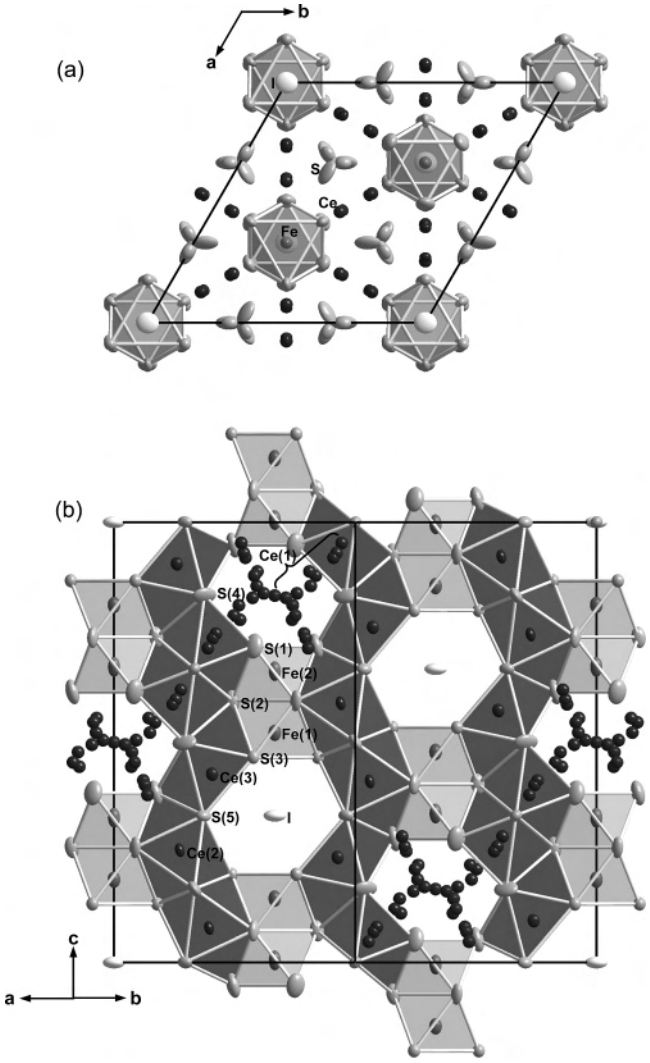

Figure 2. $Ce_{53}Fe_{12}S_{90}I_3$ structure viewed (a) along [001] and (b) as a (110) section. For clarity, only the most populated Ce(1) site, Ce(1b), is shown in part a. The atomic labeling scheme is indicated in part b. Displacement ellipsoids are drawn at the 90% probability level.

the structure contains Fe_2S_9 dimers of face-sharing octahedra, which are stacked along the $\bar{3}$ axes of the cell. The dimers are linked by face- and vertex-sharing capped CeS_6 trigonal prisms to form a three-dimensional metal sulfide framework encompassing large cuboctahedral cavities. Two types of cavities alternate along the $\bar{3}$ axes, separating the Fe_2S_9 dimers. The smaller cavities accommodate alternative sites for disordered cerium atoms. The larger cavities, which are empty in the parent structure, are filled by iodide anions.

The Fe_2S_9 dimers are face-sharing bioctahedra containing two independent iron atoms (Figure 3a). The $Fe(1)S(2)_3S(3)_3$ and $Fe(2)S(1)_3S(2)_3$ octahedra are both trigonally compressed along [001], and the central iron atoms are shifted away from the shared triangular face. The bridging Fe(1)−S(2) and Fe(2)−S(2) distances of 2.641(3) and 2.567(3) Å are considerably longer than the terminal Fe(1)−S(3) and Fe(2)−S(1) distances of 2.466(3) and 2.414(4) Å, indicating a repulsive interaction between the iron cations. The resulting Fe(1)···Fe(2) distance of 3.081(4) Å is somewhat longer than the Fe···Fe separation of 2.980(6) Å

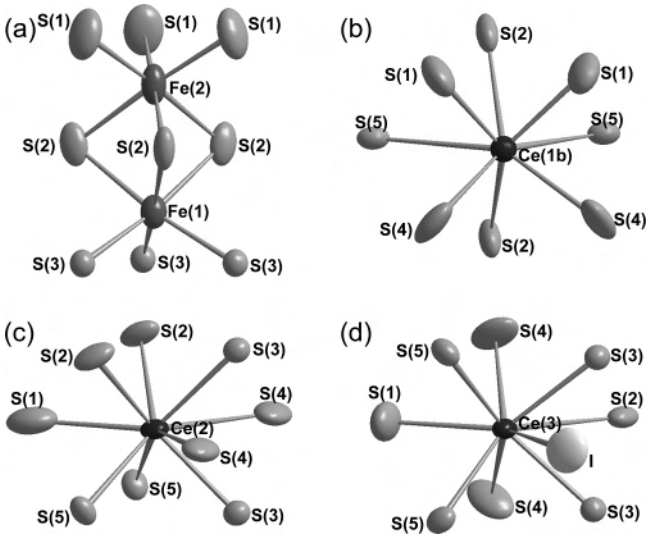

Figure 3. Metal atom coordination environments in $Ce_{53}Fe_{12}S_{90}I_3$: (a) octahedral coordination of Fe(1) and Fe(2) in a face-sharing dimer; capped trigonal-prismatic coordination of (b) Ce(1b), (c) Ce(2), and (d) Ce(3). Displacement ellipsoids are drawn at the 90% probability level.

in the $[FeS_{6/2}]$ chains of $Ce_3Fe_{1.94}S_7$.[7] The Fe−S bond lengths are comparable to those observed in the FeS_6 octahedra of other Fe^{II} compounds, for example, $La_2Fe_2S_5$ (2.45−2.67 Å)[4] or FeS (2.360−2.717 Å).[21]

The Fe_2S_9 dimers share all of their vertexes and their 12 lateral faces with sulfur coordination polyhedra centered by Ce(2), Ce(3), and the most populated Ce(1) site, Ce(1b). If some longer capping distances are accepted, the polyhedra depicted in parts b−d of Figure 3 can be described as bi- or tricapped trigonal prisms (or, alternatively, as square antiprisms or monocapped square antiprisms). Ce(1b) and Ce(3) are each coordinated by eight sulfur atoms at distances of 2.747−3.350 and 2.895−3.800 Å, respectively, and Ce(2) is coordinated by nine sulfur atoms at distances of 2.848−3.547 Å. Similarly, large ranges of Ce−S distances are found in $Ce_3Fe_{1.94}S_7$ (2.843−3.414 Å)[7] or $Ce_{10}S_{14}O$ (2.812−3.956 Å).[20] The $Ce(1b)S(1)_2S(2)_2S(4)_2S(5)_2$ and $Ce(3)S(1)S(2)S(3)_2S(4)_2S(5)_2$ prisms each share one face, and the $Ce(2)S(1)S(2)_2S(3)_2S(4)_2S(5)_2$ prisms two faces, with an Fe_2S_9 dimer. All share a vertex with a neighboring dimer as well, in addition to sharing faces and vertexes with one another. The result is a three-dimensional metal sulfide framework that contains cuboctahedral cavities of two different sizes on the $\bar{3}$ axes of the cell (Figure 2b). Smaller cavities with a volume of 113 $Å^3$ outlined by six S(1) and six S(4) atoms enclose the 3b sites, and larger cavities with a volume of 135 $Å^3$ outlined by six S(3) and six S(5) atoms enclose the 3a sites (volumes calculated for the polyhedra defined by the atom centers using *VOID95*[29]). Both cuboctahedral cavities are compressed in the [001] direction.

The position at the center of the trigonal prism that forms the square faces of the smaller cuboctahedral cavity is nonideal for a cerium atom because the Ce(1b) site is located at a short distance of 3.57(2) Å from another symmetry-

(29) Koch, E.; Fischer, W. *VOID95*; Philipps-Universität Marburg: Marburg, Germany, 1995.

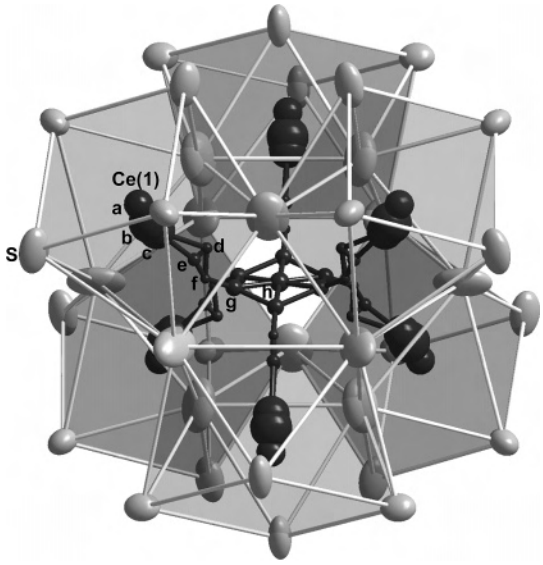

Figure 4. Positional disorder of Ce(1) in $Ce_{53}Fe_{12}S_{90}I_3$. A path of eight closely spaced sites, Ce(1a−h), extends from the framework into the neighboring cavity. The size of the Ce(1a−h) atoms at each site represents their occupancy, and the lines connecting them represent possible paths between the sites. The total occupancy of the sites is $^{17}/_{18}$. Displacement ellipsoids of other atoms are drawn at the 90% probability level.

generated Ce(1b) site [if the Ce(1b) coordination polyhedra are described as square antiprisms, the two polyhedra share a square face]. The cerium atoms, therefore, shift their positions to avoid this close contact and occupy a path of eight closely spaced sites [Ce(1a−h)] that extends into the neighboring cavity, as shown in Figure 4. The total occupancy of these sites is $^{17}/_{18}$, with the vacancies being required for charge balance according to the formula $(Ce^{3+})_{53}\square_1(Fe^{2+})_{12}(S^{2-})_{90}(I^-)_3$. The sites just outside of the cavity, Ce(1a−c), which have a combined occupancy of approximately 80%, have bicapped trigonal-prismatic (or square-antiprismatic) surroundings similar to those of Ce(2) and Ce(3). However, the inner sites, which each have occupancies between 2 and 8%, have more unusual and highly distorted coordination environments. Sites Ce(1d−f) are coordinated by square pyramids of five sulfur atoms, site Ce(1g) by a monocapped trigonal prism of seven sulfur atoms, and site Ce(1h), at the center of the cavity, by an octahedron of six sulfur atoms. These sites can be regarded as local energy minima on the path between the more stable positions Ce(1a−c). The partial filling of the cavities surrounding the 3b sites by cations results in their smaller size.

The 3a sites at the centers of the larger cavities are occupied by iodine atoms, which serve as third capping atoms for the trigonal prisms centered by Ce(3) (Figure 3c). The Ce−I distance of 3.7497(9) Å is rather long when compared to those observed in the capped trigonal prisms of the two known cerium sulfide iodides, CeSI (3.27−3.47 Å)[30] and $Ce_3(SiS_4)_2I$ (3.2954−3.4324 Å).[31] However, the large displacement parameter of this atom is an indication of its tendency to shift away from the cavity center and closer to the neighboring cerium atoms.

Structural Variations with X. The cell parameters of $Ce_{52}Fe_{12}S_{90}$ and $Ce_{53}Fe_{12}S_{90}X_3$ (X = Cl, Br, I) are plotted in Figure 1. As expected, an increase in volume occurs upon insertion of the halogen atoms into the unfilled parent structure $Ce_{52}Fe_{12}S_{90}$. This cell expansion is realized through a lengthening of the *c* parameter, which increases with the size of the halogen atom. The *a* parameter, on the other hand, remains relatively constant, increasing slightly upon insertion of chlorine or bromine atoms and decreasing slightly upon insertion of iodine atoms. Consequently, the volume of $Ce_{53}Fe_{12}S_{90}X_3$ expands from X = Cl to Br but contracts slightly from X = Br to I.

These changes originate from the combined effects of anion−anion S···X repulsion and Ce−X bonding in the filled structure. As discussed above, the cuboctahedral cavity that accommodates the halogen atom is compressed along the *c* direction. To minimize unfavorable S···X interactions, it is necessary for the height of the cavity, and hence the length of the *c* parameter, to increase significantly upon halogen-atom insertion. However, the expansion of the cavity is counterbalanced by the need to establish Ce−X and Ce−S bonds of appropriate lengths. In $Ce_{53}Fe_{12}S_{90}Cl_3$ and $Ce_{53}Fe_{12}S_{90}Br_3$, an off-center displacement of the smaller halogen atoms allows the formation of Ce−Cl bonds of 3.17-(2) or 3.48(2) Å and Ce−Br bonds of 3.332(9) or 3.520(7) Å. The shorter distances are similar to those reported for $Ce_3(SiS_4)_2Cl$ (2.934−3.297 Å) and $Ce_3(SiS_4)_2Br$ (3.125−3.329 Å).[32] This displacement, which has its largest components in the *ab* plane, causes a small increase in the width of the cavity and a corresponding lengthening of the *a* parameter.

Structural Relationships. The structure of the $Ce_{53}Fe_{12}S_{90}X_3$ compounds is closely related to the Mn_5Si_3 structure type.[16] This structure type is widespread, being adopted by hundreds of combinations of metals and metalloids.[33] The Mn_5Si_3 structure is also a versatile host that can accommodate a wide range of atoms in octahedral interstitial sites to give ternary compounds of composition A_5B_3Z with the same basic structure and space group ($P6_3/mcm$).[17] While most of the filled and unfilled Mn_5Si_3-type compounds are metal-rich, the compounds R_3MSb_5 (R = La, Ce, Pr, Nd, Sm, U; M = Ti, Zr, Hf, V, Nb, Cr, Mn) adopt an anti-type structure.[34,35] The structure of one representative, La_3TiSb_5, is depicted in Figure 5a,b. In this structure, a $[TiSb(1)_{6/2}]$ chain of face-sharing octahedra propagates along the 6_3 axis at (0, 0, *z*). The Sb(2) atoms form linear chains that follow the $\bar{6}$ axes at ($^1/_3$, $^2/_3$, *z*) and ($^2/_3$, $^1/_3$, *z*). The lanthanum atoms,

(30) Etienne, J. *Bull. Soc. Fr. Miner. Cristallogr.* **1969**, *92*, 134−140.
(31) Gauthier, G.; Kawasaki, S.; Jobic, S.; Macaudière, P.; Brec, R.; Rouxel, J. *J. Mater. Chem.* **1998**, *8*, 179−186.
(32) Riccardi, R.; Gout, D.; Gauthier, G.; Guillen, F.; Jobic, S.; Garcia, A.; Huguenin, D.; Macaudière, P.; Fouassier, C.; Brec, R. *J. Solid State Chem.* **1999**, *147*, 259−268.
(33) Villars, P. *Pearson's Handbook Desk Edition: Crystallographic Data for Intermetallic Phases*; ASM International: Materials Park, OH, 1997.
(34) Bolloré, G.; Ferguson, M. J.; Hushagen, R. W.; Mar, A. *Chem. Mater.* **1995**, *7*, 2229−2231.
(35) Brylak, M.; Jeitschko, W. *Z. Naturforsch., B: Chem. Sci.* **1994**, *49*, 747−752.

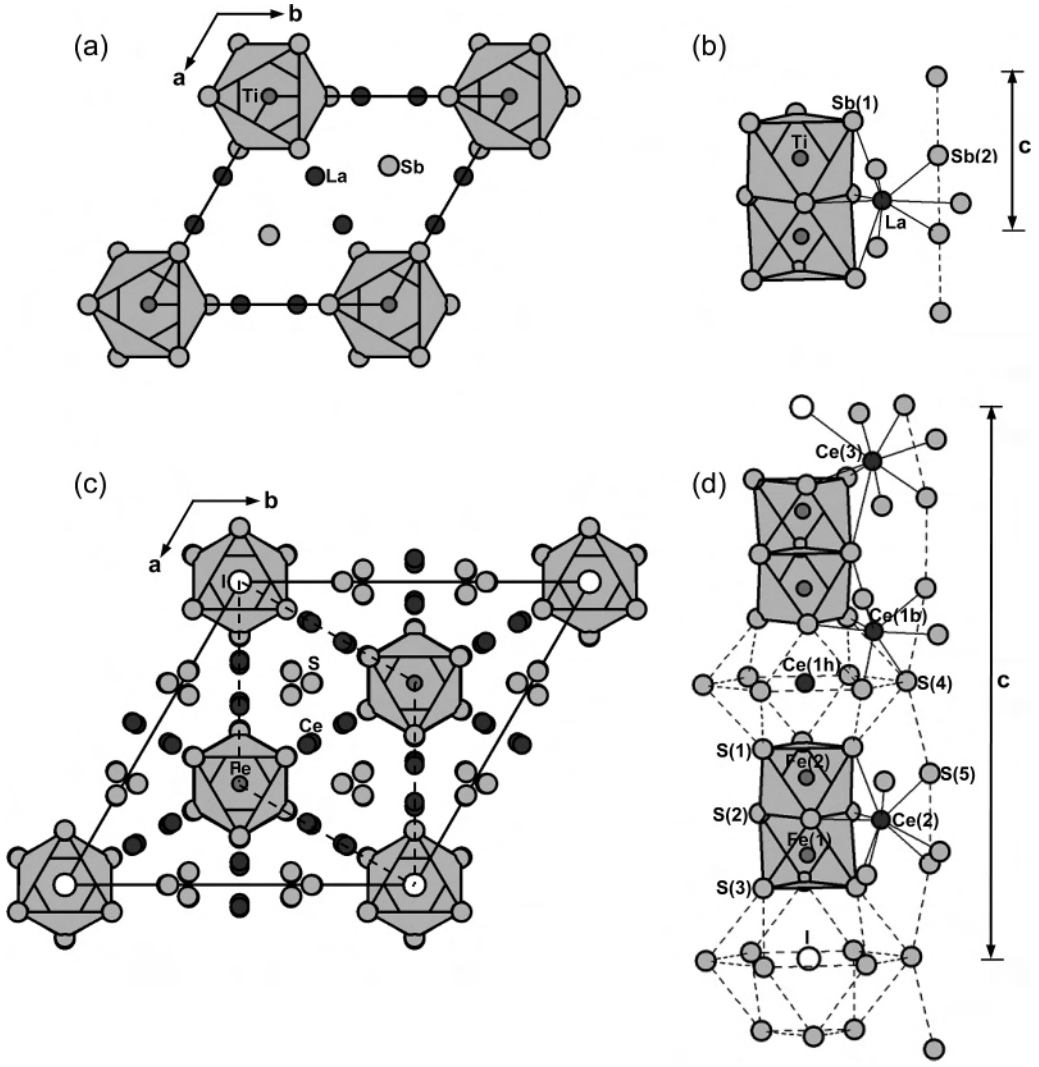

Figure 5. Comparison of the La_3TiSb_5 structure ($P6_3/mcm$) and the $Ce_{53}Fe_{12}S_{90}I_3$ superstructure ($R\bar{3}m$): views of La_3TiSb_5 along (a) [001] and (b) [110]; views of $Ce_{53}Fe_{12}S_{90}I_3$ along (c) [001], with dashed lines outlining the La_3TiSb_5 subcell, and (d) [1$\bar{1}$0].

situated in tricapped trigonal prisms of five Sb(1) and four Sb(2) atoms, link the two sets of chains.

The $Ce_{53}Fe_{12}S_{90}X_3$ compounds adopt a 9-fold trigonal superstructure of Mn_5Si_3 or R_3MSb_5, with $a = \sqrt{3}a'$ and $c = 3c'$. The structures of La_3TiSb_5 ($P6_3/mcm$) and $Ce_{53}Fe_{12}S_{90}I_3$ ($R\bar{3}m$) are compared in Figure 5, and a simplified Bärnighausen tree describing the symmetry relations between them is presented in Figure 6. The superstructure is the result of a diversification of the atoms filling the octahedral interstitial sites of the Mn_5Si_3 structure. In $Ce_{53}Fe_{12}S_{90}I_3$, iron atoms fill two-thirds of the sites, in pairs, iodine atoms fill one-sixth of the sites, and cerium atoms partially occupy the remaining sites, whereas in La_3TiSb_5, titanium atoms fill all of the sites. As can be judged by comparing parts b and d of Figure 5, the removal of every third transition-metal atom elongates the octahedra surrounding the 3a and 3b sites, resulting in cuboctahedral cavities that can accommodate anions or larger cations. The 3a sites are fully occupied by iodine atoms, and the 3b sites are partially occupied by Ce(1h) atoms. Meanwhile, the formation of Fe_2S_9 dimers compresses the octahedra surrounding the 6c sites occupied by Fe(1) and Fe(2). The rest of the

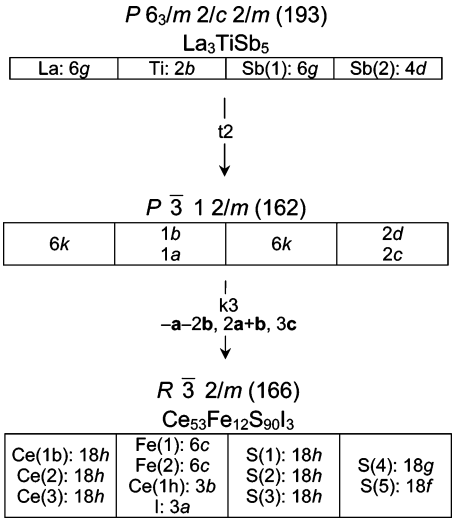

Figure 6. Simplified Bärnighausen tree describing the symmetry relations between the La_3TiSb_5 structure ($P6_3/mcm$) and the $Ce_{53}Fe_{12}S_{90}I_3$ superstructure ($R\bar{3}m$).

structure also undergoes complex adjustments to accommodate this distortion. The S(4) and S(5) atoms derived from the Sb(1) sites are now arranged in undulated, rather than

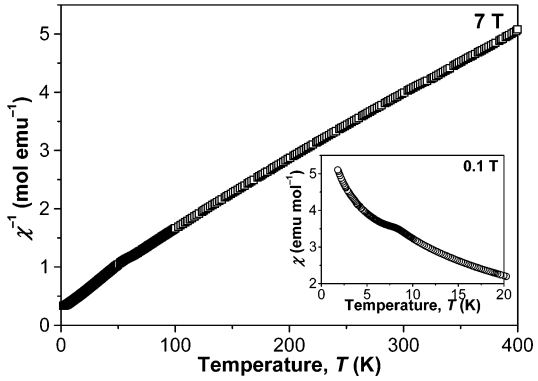

Figure 7. Temperature dependence of the reciprocal magnetic susceptibility (χ^{-1}) of $Ce_{53}Fe_{12}S_{90}I_3$ at a field of 7 T. The inset highlights the low-temperature region of the $\chi(T)$ curve measured at a field of 0.1 T.

linear, columns. This change, in addition to the shifts of S(1), S(2), and S(3) required for the formation of alternating cavities and dimers, results in different coordination environments for the framework Ce(1b), Ce(2), and Ce(3) atoms.

Magnetic Properties. The temperature dependence of the reciprocal magnetic susceptibility (χ^{-1}) of $Ce_{53}Fe_{12}S_{90}I_3$ between 2 and 400 K at a field of 7 T (the very high field was used to suppress the signal of a minor ferromagnetic impurity) is shown in Figure 7. At higher temperatures, the $\chi^{-1}(T)$ plot is approximately linear, but it changes slope near 60 K and then departs from linearity. A fit of the data between 100 and 400 K to the Curie−Weiss law yields an effective magnetic moment μ_{eff} of 25.05(3) μ_B, per $Ce_{53}Fe_{12}S_{90}I_3$ formula unit, which is very close to the value of 25.1 μ_B calculated from the theoretical moments of Ce^{III} (2.54 μ_B) and high-spin Fe^{II} (spin-only, 4.90 μ_B), and a Weiss parameter θ of −30.5(1) K, which suggests antiferromagnetic exchange interactions. At low fields (below 1 T), a broad peak in the $\chi(T)$ curve, which may be an indication of a transition to an antiferromagnetically ordered state, is observed at approximately 8 K (inset to Figure 7). Further experiments will be required to verify this hypothesis.

Acknowledgment. We thank Dr. Walter Schnelle (Max-Planck-Institut für Chemische Physik fester Stoffe) for making the magnetic measurements and D. Bräunling, G. Kadner, and J. Krug (Technische Universität Dresden) for experimental help. We gratefully acknowledge the financial support of the Deutsche Forschungsgemeinschaft (DFG) within the SFB 463.

Supporting Information Available: Structural data as CIF files. This material is available free of charge via the Internet at http://pubs.acs.org.

IC0521372